

---

# GraphXForm: Graph transformer for computer-aided molecular design with application to extraction

---

Jonathan Pirnay<sup>\*12</sup> Jan G. Rittig<sup>\*3</sup> Alexander B. Wolf<sup>\*4</sup> Martin Grohe<sup>5</sup> Jakob Burger<sup>4</sup>  
Alexander Mitsos<sup>637</sup> Dominik G. Grimm<sup>12</sup>

## Abstract

Generative deep learning has become pivotal in molecular design for drug discovery and materials science. A widely used paradigm is to pretrain neural networks on string representations of molecules and fine-tune them using reinforcement learning on specific objectives. However, string-based models face challenges in ensuring chemical validity and enforcing structural constraints like the presence of specific substructures. We propose to instead combine graph-based molecular representations, which can naturally ensure chemical validity, with transformer architectures, which are highly expressive and capable of modeling long-range dependencies between atoms. Our approach iteratively modifies a molecular graph by adding atoms and bonds, which ensures chemical validity and facilitates the incorporation of structural constraints. We present GraphXForm, a decoder-only graph transformer architecture, which is pretrained on existing compounds and then fine-tuned using a new training algorithm that combines elements of the deep cross-entropy method with self-improvement learning from language modeling, allowing stable fine-tuning of deep transformers with many layers. We evaluate GraphXForm on two solvent design tasks for liquid-liquid extraction, showing that it outperforms four state-of-the-art molecular design techniques, while it can flexibly enforce structural constraints or initiate the design from existing molecular structures.

## 1. Introduction

Molecular design plays an important role across many fields, such as drug discovery, materials science, and chemical en-

gineering. The immense chemical search space, estimated to contain between  $10^{60}$  and  $10^{100}$  potential molecules (Schneider & Fechner, 2005), renders manual approaches to molecular design both arduous and resource-intensive.

Advancements in deep learning have significantly impacted molecular design, enabling efficient navigation of the chemical space with the help of neural networks (Fu et al., 2022; Gómez-Bombarelli et al., 2018; Segler et al., 2018; Bjerum & Threlfall, 2017; Zhang et al., 2023a). A prevalent paradigm is to represent molecules as strings of text, such as SMILES (Weininger, 1988) or SELFIES (Krenn et al., 2020), and use neural network architectures from language modeling, such as recurrent neural networks (RNNs) or transformers (Vaswani, 2017), to generate novel molecular structures. These architectures are typically pretrained on large datasets of existing molecules to learn general underlying patterns in the strings and then fine-tuned on specific objective functions via reinforcement learning (RL) for downstream tasks (Olivecrona et al., 2017; Gao et al., 2022; Xu et al., 2024; Mazuz et al., 2023; Gupta et al., 2018).

To address the challenge of capturing long-range dependencies in sequential data that RNNs face, transformers (Vaswani, 2017) have been successfully applied due to their ability to model long-range dependencies more efficiently and as they are widely used in language modeling today (Xu et al., 2024). However, transformers are resource-intensive, and needing to fine-tune them with RL can limit the size that is used in practice (Xu et al., 2024; Henderson et al., 2018; Schulman et al., 2017). In general, chemical language models may propose string representations of molecules with invalid chemical structures – for example, when SMILES syntax or valence constraints are violated – which has led to numerous works aimed at circumventing this problem (O’Boyle & Dalke, 2018; Krenn et al., 2020; Cheng et al., 2023; Dai et al., 2018). Despite recent evidence that invalid SMILES can actually be beneficial from a language modeling perspective (Skinnider, 2024), they can harm the RL component of the pipeline as they can increase sample complexity and necessitate reward shaping to account for them. Additionally, the sequential nature of string synthesis makes it difficult to enforce structural constraints, such as

---

<sup>\*</sup>Equal contribution <sup>1</sup>Technical University of Munich, TUM Campus Straubing for Biotechnology and Sustainability, Bioinformatics, Straubing <sup>2</sup>University of Applied Sciences Weihenstephan-Triesdorf, Bioinformatics, Straubing <sup>3</sup>Process Systems Engineering (AVT.SVT), RWTH Aachen University, Aachen <sup>4</sup>Technical University of Munich, TUM Campus Straubing for Biotechnology and Sustainability, Laboratory of Chemical Process Engineering, Straubing <sup>5</sup>Chair of Computer Science 7, RWTH Aachen University, Aachen <sup>6</sup>JARA Center for Simulation and Data Science (CSD), Aachen <sup>7</sup>Forschungszentrum Jülich GmbH, Institute of Climate and Energy Systems ICE-1: Energy Systems Engineering, Jülich. Correspondence to: Dominik G. Grimm <dominik.grimm@hswt.de>.

ensuring the presence of a minimum number of specific atom types, restrictions on bonds, or even enforcing the presence of certain substructures within the molecules.

An alternative approach is to represent molecules directly as graphs, where atoms are nodes and bonds are edges, and to develop models that modify a molecular graph or design it directly (Wang et al., 2023; Li et al., 2018; Jin et al., 2018; Zhou et al., 2019; Jensen, 2019; De Cao & Kipf, 2018; Zang & Wang, 2020; Zhang et al., 2023b; Mahmood et al., 2021; Maziarka et al., 2019; Rittig et al., 2023d). Working at the graph level, allows explicit encoding of atomic interactions and bonding rules, ensuring chemical validity, and makes it straightforward to start from existing structures and modify them. For example, graph-based methods like GraphGA (Jensen, 2019) employ genetic algorithms to modify molecular graphs directly, even outperforming several neural-based string-synthesis methods without relying on neural networks. As a deep learning example, Zhou et al. (2019) use deep Q-Learning (Mnih, 2013) with a simple feedforward network to optimize graphs from scratch by adding or removing atoms and bonds.

We propose to combine and extend the strengths of both paradigms: employing transformers for their ability to capture long-range dependencies in sequence data, and leveraging pretraining on existing molecules, all while working directly on the molecular graph. More specifically, we use graph transformers (Ying et al., 2021; Maziarka et al., 2019) and formulate molecule design as a sequential task, where a molecular graph – starting from an arbitrary structure – is iteratively extended by placing atoms, bonding them to existing atoms, and modifying the graph by increasing bond orders.

To this end, we introduce GraphXForm, a decoder-only graph transformer architecture that guides these incremental decisions, predicting the next action based on the current molecular graph. Pretrained on existing compounds, GraphXForm employs a novel fine-tuning approach that combines elements of the deep cross-entropy method (Wagner, 2021) and self-improvement learning (Huang et al., 2023; Pirnay & Grimm, 2024a). Unlike commonly used deep reinforcement learning methods like REINFORCE (Williams, 1992), this approach allows for stable training of deep transformers with many layers.

We test GraphXForm for the design of solvents, which are highly relevant for chemical processes. While algorithmic advances in molecular design have primarily focused on *de novo* drug development, other areas such as materials science and chemical engineering have only recently gained attention. Recent applications include catalyst (Schilter et al., 2023), fuel (Rittig et al., 2023d; Sarathy & Eraqi, 2024), polymer (Jiang et al., 2024; Yue et al., 2024), surfactant (Nnadili et al., 2024), chemical reaction substrate (Nigam

et al., 2023), and solvent (König-Mattern et al., 2024) design. We focus specifically on solvents due to their vital role in industrial chemical processes such as reactions, separations, and extractions. While König-Mattern (König-Mattern et al., 2024) recently applied a graph-based genetic algorithm for solvent design, the use of generative ML-based approaches remains underexplored. Therefore, our goal is to compare newer design methods and expand their capabilities.

We evaluate GraphXForm on two liquid-liquid extraction tasks. The objective function in these tasks is defined by a separation factor based on activity coefficients at infinite dilution. We compare GraphXForm on these two downstream tasks to four state-of-the-art molecular design approaches (Graph GA (Jensen, 2019), REINVENT-Transformer (Xu et al., 2024), Junction Tree VAE (Jin et al., 2018), and STONED (Nigam et al., 2021)). Additionally, we demonstrate GraphXForm’s unique flexibility and stability by incorporating structural constraints conceptually suited for solvent design, such as preventing certain bond types or preserving complex molecular substructures, allowing us to design solvents with highly tailored properties. This capability highlights the strength of our approach in tackling design tasks that are difficult or infeasible for existing methods.

Our contributions are summarized as follows:

- **We formulate molecular design as a sequential task**, where an initial structure (e.g., a single atom) is iteratively modified by adding atoms and bonds.
- **We introduce a graph transformer architecture** that takes a molecular graph as input and outputs probability distributions for atom placement and bond modification. This approach maintains the notion of using transformers for molecular design while moving away from string-based methods.
- **We propose a training algorithm** that enables the stable and efficient fine-tuning of deep graph transformers on downstream tasks.
- **We demonstrate that our method outperforms state-of-the-art molecular design techniques** on two solvent design tasks and can be easily adapted to satisfy structural constraints or preserve specific molecular structures.

Our code for pretraining and fine-tuning is available at: <https://github.com/grimmlab/graphxform>.

## 2. Methods and Modeling

In this section, we introduce GraphXForm. In Section 2.1, we formally set up the molecular design task as the sequential construction of a graph. As in a deep reinforcement

learning setup, the goal is to find a policy network that guides these sequential decisions. In Section 2.2, we introduce our algorithm for training the policy network, before describing the used transformer architecture in Section 2.3.

## 2.1. Molecular design

**Molecular graph** In the following, we represent a molecule by its hydrogen-suppressed graph representation, where nodes correspond to atoms and edges correspond to bonds. For ease of notation, we assume an arbitrary ordering over the nodes. Let  $\Sigma = (\Sigma_1, \dots, \Sigma_k)$  be an underlying alphabet of possible atom types. We represent a molecule with  $n$  atoms by a pair  $(\mathbf{a}, \mathbf{B})$ , where  $\mathbf{a} = (a_1, \dots, a_n) \in \{1, \dots, k\}^n$  and  $a_i$  indicates that the  $i$ -th node is of atom type  $\Sigma_{a_i}$ . The matrix  $\mathbf{B} = (B_{ij})_{1 \leq i, j \leq n} \in \mathbb{N}_0^{n \times n}$  represents the bonds and their orders between atoms, i.e., we have that  $B_{ij} \in \mathbb{N}_0$  is the bond order between the  $i$ -th and the  $j$ -th atom. In particular,  $\mathbf{B}$  is symmetric with zero diagonal and nonzero columns and rows (i.e., each atom is connected to at least one other atom and not to itself). For example, given the alphabet  $\Sigma = (\text{C}, \text{N}, \text{O})$  the molecule with SMILES representation C=O can be given as  $(\mathbf{a}, \mathbf{B})$  with  $\mathbf{a} = (1, 3)$  and  $\mathbf{B} = \begin{pmatrix} 0 & 2 \\ 2 & 0 \end{pmatrix}$ .

We denote by  $\mathcal{M}'$  the space of all molecular graphs  $m = (\mathbf{a}, \mathbf{B})$  as described above. Accordingly, let  $\mathcal{M} \subset \mathcal{M}'$  be the subspace of molecular graphs that are chemically valid, i.e., all non-hydrogen atoms follow the octet rule. We refer to following the octet rule as satisfying the 'valence constraints' throughout the paper.

**Sequential molecular graph design** Similar to Zhou et al. (2019), we pose molecular design as a sequential Markov decision process (MDP), where an agent assembles a molecular graph by iteratively adding atoms or increasing the bond order between atoms. We note that in the graph, hydrogens are always only considered implicitly, and an addition of an atom or a bond leads to a replacement of an implicit hydrogen.

On a high level, a single molecule is constructed by the agent as follows: The agent observes an initial molecule  $m^{(0)}$ , and then performs some *action*  $x^{(0)}$  on it, which results in a new molecule  $m^{(1)}$ . Then, the agent observes  $m^{(1)}$ , decides on an action  $x^{(1)}$  leading to molecule  $m^{(2)}$ , and so on. This iterative design process terminates at some molecule  $m^{(T)}$  once the agent decides to perform a special DONTCHANGE action, which does not alter the molecular graph but rather marks the design as *finished*.

We formalize this as follows: Let  $m^{(t)} = (\mathbf{a}^{(t)}, \mathbf{B}^{(t)})$  be some molecule with atoms  $\mathbf{a}^{(t)} \in \{1, \dots, k\}^{n^{(t)}}$  and bond matrix  $\mathbf{B}^{(t)} \in \mathbb{N}_0^{n^{(t)} \times n^{(t)}}$  as above. We transition to a new

molecule  $m^{(t+1)} = (\mathbf{a}^{(t+1)}, \mathbf{B}^{(t+1)})$  by performing some *action*  $x^{(t)} \in \mathcal{A}$  on  $m^{(t)}$ . An action  $x^{(t)}$  in the action space  $\mathcal{A}$  is of one of the following three types:

1.  $x^{(t)} = \text{DONTCHANGE}$ , which terminates the design of the molecule. In particular,  $m^{(t+1)} = m^{(t)}$  and  $n^{(t+1)} = n^{(t)}$ .
2.  $x^{(t)} = \text{ADDATOM}(j, l)$ , with  $j \in \{1, \dots, k\}$  and  $l \in \{1, \dots, n^{(t)}\}$ . This action adds an atom of type  $\Sigma_j$  to the graph and bonds it to the  $l$ -th atom. In particular, we set  $n^{(t+1)} = n^{(t)} + 1$ . For the new molecule  $m^{(t+1)} = (\mathbf{a}^{(t+1)}, \mathbf{B}^{(t+1)})$ , the atom vector  $\mathbf{a}^{(t+1)} \in \mathbb{N}^{n^{(t+1)}}$  is obtained by appending  $j$  to  $\mathbf{a}^{(t)}$ . The second entry  $l \in \{1, \dots, n^{(t)}\}$  indicates that we bond this new  $(n+1)$ -th atom to the  $l$ -th atom, i.e.,  $\mathbf{B}^{(t+1)} \in \mathbb{N}_0^{n^{(t+1)} \times n^{(t+1)}}$  is obtained by appending a zero row and column to  $\mathbf{B}^{(t)}$  and setting  $B_{n+1, l}^{(t+1)} = B_{l, n+1}^{(t+1)} = 1$ .
3.  $x^{(t)} = \text{INCBOND}(j, l)$ , meaning that we are increasing the bond order between atoms  $j$  and  $l$ . In particular, we have  $n^{(t+1)} = n^{(t)}$  and  $\mathbf{a}^{(t+1)} = \mathbf{a}^{(t)}$ . The bond matrix  $\mathbf{B}^{(t+1)}$  is obtained from  $\mathbf{B}^{(t)}$  by setting  $B_{j, l}^{(t+1)} = B_{l, j}^{(t+1)} = B_{j, l}^{(t)} + 1$ . Note that this allows not only higher order bonds, but also bonds between previously unbonded atoms.

Given a molecule  $m^{(0)}$  and a sequence of actions  $x^{(0)}, \dots, x^{(t-1)}$ , we will also write  $(m^{(0)}, x^{(0)}, \dots, x^{(t-1)})$  for the molecule  $m^{(t)} \in \mathcal{M}$  that results from  $m^{(0)}$  by sequentially applying the actions  $x^{(0)}, \dots, x^{(t-1)}$  to  $m^{(0)}$ . We note that, in general, the action sequence  $x^{(0)}, \dots, x^{(t-1)}$  is not unique to from  $m^{(0)}$  to  $m^{(t)}$ .

Starting from a molecule in  $\mathcal{M}$ , by removing chemically invalid actions from the action space (which would lead to violation of valence constraints) at each step, we can guarantee to stay in the space of chemically valid molecules. Once the agent chooses the DONTCHANGE action, the design process is considered finished. We note that, starting from an appropriate initial atom, it is in fact possible to reach every target molecule in the chemically valid space  $\mathcal{M}$  (i.e., all molecular graphs that can be constructed from the alphabet  $\Sigma$  and that satisfy the valence constraints) when starting from any atom that exists in the target molecule. For an illustrative molecule construction, see Fig. 1.

Each addition of a bond or atom removes an implicit hydrogen from the respective atom, allowing for a straightforward representation of ionization states: Ions can be incorporated simply by adding charged atom types to the predefined alphabet, without the need for additional modifications to the action space. In contrast, the graph-based approach can not handle stereochemistry in a straightforward way.

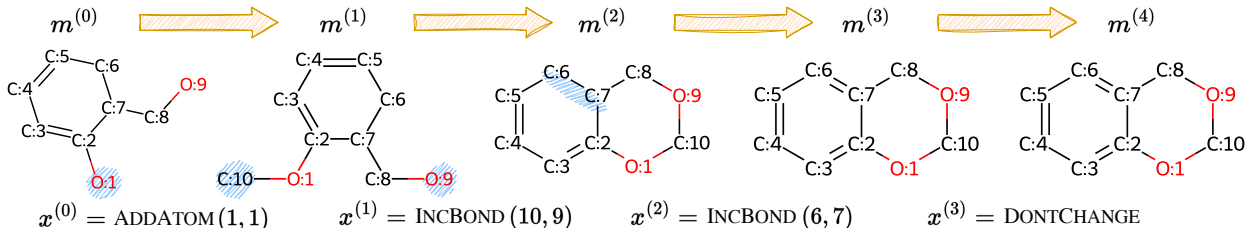


Figure 1. Example for the sequential application of actions  $x^{(0)}, \dots, x^{(3)}$  to a molecule  $m^{(0)}$ , using the alphabet  $\Sigma = (C, N, O)$ . We show the index of each atom, which can be arbitrarily chosen at the beginning. Light blue indicates where in the graph an action is applied. The last action is DONTCHANGE, which does not change the molecular graph, but marks it as a finished design.

**Molecular optimization** Formally, we aim to design molecules

$$m^* \in \arg \max_{m \in \mathcal{M}} f(m) \quad (1)$$

that maximize a predefined objective function  $f: \mathcal{M}' \rightarrow \mathbb{R} \cup \{-\infty\}$ , where chemically invalid molecules are mapped to  $-\infty$ . As in previous work (Mazuz et al., 2023; Zhou et al., 2019; Xu et al., 2024), we pose the corresponding learning problem to (1) in the terms of deep RL: the agent’s decision at each step is guided by a *policy* that maps a chemically valid molecule to a probability distribution over possible actions. The policy is modeled by a neural network: We write  $\pi_\theta: \mathcal{M} \rightarrow \Delta \mathcal{A}$  for a policy depending on network parameters  $\theta$ , that maps a valid molecule  $m \in \mathcal{M}$  to a probability distribution  $\pi_\theta(m)$  over  $\mathcal{A}$ . The goal is to find  $\pi_\theta$  that, given any initial molecule  $m^{(0)}$ , maximizes the expectation

$$\mathbb{E}_{\substack{x^{(0)}, \dots, x^{(T)} \\ x^{(T)} = \text{DONTCHANGE}}} \sim \pi_\theta \left[ f \left( (m^{(0)}, x^{(0)}, \dots, x^{(T)}) \right) \right], \quad (2)$$

where the expectation is taken over finished molecules sampled from  $\pi_\theta$ .

**Satisfying constraints** To ensure chemical validity at every step of the molecule design process, we mask any action in the policy that would lead to a violation of valence constraints. That means, that we set the corresponding probability to zero in the distribution predicted by the policy (before re-normalizing the distribution).

Our graph-based approach allows us to extend this concept of action masking to enforce additional constraints, such as particular bonding patterns, minimum/maximum number of atoms and their types, or the presence of structural motifs like rings. We explore these constraints in detail in Section 3. We note that it is possible to simply assign an objective value of  $-\infty$  to molecules that violate these constraints *after* the design process. However, the ability to preemptively avoid constraint-violating regions by masking actions *during* the design process can significantly reduce the search space. In contrast, methods that generate molecules by sequentially

synthesizing SMILES (Gupta et al., 2018; Xu et al., 2024; Mazuz et al., 2023) strings struggle to enforce such constraints during the construction process while also adhering to the grammatical rules of SMILES.

## 2.2. Learning algorithm

We now introduce our method for training the policy neural network  $\pi_\theta$ . Our proposed learning algorithm is a hybrid of the deep cross-entropy method (CEM) (Wagner, 2021) and the self-improvement learning (SIL) (Huang et al., 2023; Corsini et al., 2024; Pirnay & Grimm, 2024a;b) strategy. Both approaches train the network over multiple epochs in a self-improving loop, where, in each epoch, the current policy is used to generate a set of action sequences. The best sequences are selected as ‘pseudo-labels’, i.e., they serve as the dataset for *supervised* training. The network is then trained for one epoch to assign higher probabilities to these sequences before the process is repeated with the updated network to generate new action sequences. Unlike other deep RL algorithms, this approach does not require reward shaping or value approximation. Furthermore, training in a supervised way provides stability and allows for the use of larger, decoder-only transformer architectures (Vaswani, 2017), which would be prohibitively slow under standard RL. However, SIL and the deep CEM differ in key aspects: The deep CEM is formulated for problems with a *single* instance (as in our molecular design task) and retains a certain percentage of the best action sequences in each epoch, which are obtained through simple sampling from the policy’s predicted distributions at each step. SIL, on the other hand, is typically applied to problems with *infinitely* many instances and employs more advanced sequence decoding techniques, such as sequence sampling without replacement (Kool et al., 2019), to improve solution quality and diversity while maintaining efficient decoding speed.

In our proposed approach, we aim to develop a method that works for single-instance problems, as in the deep CEM, while retaining the diverse sampling mechanism used in SIL methods (Pirnay & Grimm, 2024a;b). The pseudocode for

our approach is presented in Algorithm 1, and we describe the key steps below:

1. We begin with a policy network  $\pi_\theta$ . The parameters  $\theta$  can be initialized randomly or, e.g., pretrained in an unsupervised manner on existing molecules (see Section 3.3). Additionally, we assume an initial molecule  $m_0 \in \mathcal{M}$  in the space of chemically valid molecules  $\mathcal{M}$ , from which the construction starts. In practice, we typically choose  $m_0$  to consist of a single carbon atom.
2. Throughout the training process, we maintain a set **BESTFOUND** of the best molecules discovered, which will be returned at the end. Initially, this set contains only the starting molecule  $m_0$ .
3. In each epoch, we incrementally sample action sequences *without replacement* from the policy until either an improved molecule is found or a maximum number of samples is reached (lines 5-10). For sampling sequences without replacement, we use the efficient batch-wise incremental method introduced by Shi et al. (2020), which relates to Stochastic Beam Search (Kool et al., 2019) and is employed in SIL methods (Pirnay & Grimm, 2024a;b). Sampling without replacement ensures that unique action sequences are generated, exploring the search space effectively (especially for shorter action sequences (Shi et al., 2020)). We emphasize that, while different action sequences may lead to the same molecule, this does not pose an issue because the policy is only concerned with generating the action sequences rather than the molecular structure. Since the goal of sampling sequences without replacement is to produce distinct sequences, the policy still generates diverse outputs, even if the resulting molecules can be identical.
4. After sampling, the set **BESTFOUND** serves as a training dataset (lines 12-14). Similar to how decoder-only models in language modeling are trained to predict the next token from partial text, we sample batches of intermediate molecules and train the network with a cross-entropy loss to predict the next action for the corresponding molecule.
5. In the next epoch, the process is repeated with the updated network weights.

### 2.3. Policy network architecture

The policy network takes a molecule as input and predicts a probability distribution over next actions. To achieve this, we use a simplified version of the Graphormer (Ying et al., 2021) architecture, which treats the molecule’s atoms as an unordered sequence of nodes. This sequence is passed

---

#### Algorithm 1: Learning algorithm for molecular design

---

**Input:**  $\pi_\theta$ : Policy network with trainable parameters  $\theta$

**Input:**  $f$ : objective function to maximize

**Input:**  $m_0$ : initial molecule

**Input:**  $s \in \mathbb{N}$ : number of best molecules to keep

**Input:**  $q_{\min}, q_{\max} \in \mathbb{N}$ : minimum and maximum number of molecules to sample without replacement

```

1 BESTFOUND  $\leftarrow$   $\{m_0\}$ 
2 BESTOBJ  $\leftarrow$   $f(m_0)$ 
3 foreach epoch do
4   SAMPLED  $\leftarrow$   $\emptyset$ 
5   while  $|\text{SAMPLED}| < q_{\max}$  do
6      $m \leftarrow$  sample from  $\mathcal{M}$  with probability
7      $\pi_\theta(m \mid m_0, m \notin \text{SAMPLED})$ 
8     SAMPLED  $\leftarrow$  SAMPLED  $\cup \{m\}$ 
9     if  $f(m) > \text{BESTOBJ}$  then
10      BESTOBJ  $\leftarrow$   $f(m)$ 
11      if  $|\text{SAMPLED}| > q_{\min}$  then
12       break
13   BESTFOUND  $\leftarrow$  top  $s$  molecules in
14   BESTFOUND  $\cup$  SAMPLED
15   foreach batch do
16     uniformly sample from BESTFOUND batch of
17      $B$  (intermediate) molecules
18      $m_{t_{j+1}}^{(j)} = (m_{t_j}^{(j)}, x_{t_j}^{(j)})$  for  $j \in \{1, \dots, B\}$ 
19     minimize batch-wise cross-entropy loss
20      $L_\theta = -\frac{1}{B} \sum_{j=1}^B \log \pi_\theta(x_{t_j}^{(j)} \mid m_{t_j}^{(j)})$ 
21 return BESTFOUND

```

---

through a stack of transformer layers, with the attention mechanism augmented by bonding information. The resulting latent representations of the nodes are then used to predict action distributions. Figure 2 provides an illustration, and we elaborate on the architecture below:

**Molecular graph transformer** Let  $m = (\mathbf{a}, \mathbf{B})$  represent a molecule, where  $\mathbf{a} = (a_1, \dots, a_n) \in \mathbb{N}^n$  are the atoms, and  $\mathbf{B} \in \mathbb{N}_0^{n \times n}$  is the bond matrix. Each atom  $a_i \in \{1, \dots, k\}$  corresponds to an atom type selected from an alphabet  $\Sigma = (\Sigma_1, \dots, \Sigma_k)$ .

Following the Graphormer (Ying et al., 2021) model, we introduce a ‘virtual atom’  $a_0 = 0$  into the molecular graph, which is connected to every atom via a special ‘virtual bond’ (see Figure 2). This virtual bond is represented in the bond matrix by an integer outside the range of standard bond orders. The virtual atom functions similarly to the special [CLS]-token in BERT (Devlin, 2018) and accumulates sequence-level information for downstream tasks. Concep-

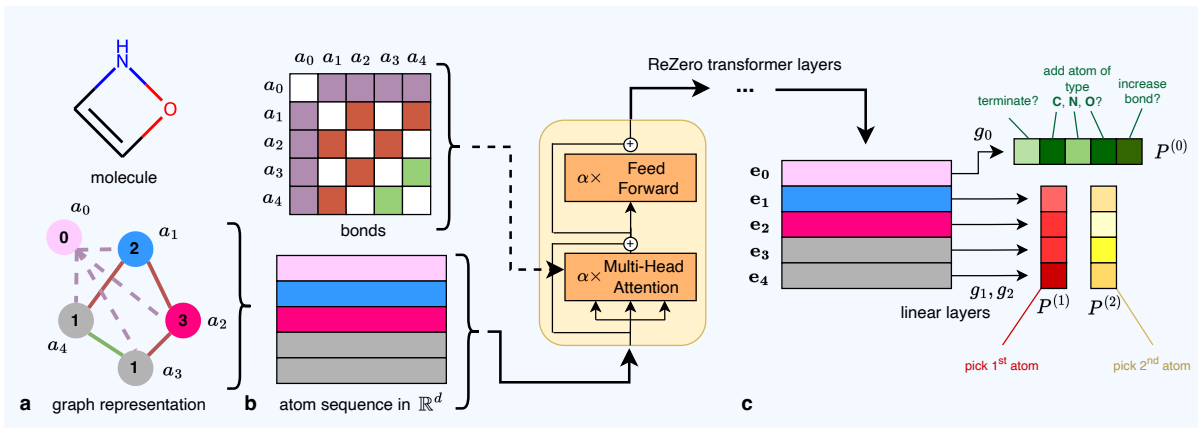


Figure 2. Flow of a molecule through the policy network of our method GraphXForm. **a**. We consider the alphabet  $\Sigma = (C, N, O)$ . The molecule’s underlying graph is augmented with a virtual node (indexed with 0) and embedded into the latent space  $\mathbb{R}^d$ . **b**. The latent sequence of atoms is passed through a stack of ReZero transformer layers, omitting positional encoding. In the multi-head attention, individual attention scores between atoms are biased with learnable scalars that depend on their bond order. These bias terms are learnable for each transformer layer and attention head individually. **c**. The sequence output by the transformer is projected through linear layers to generate logits for the distributions  $P^{(0)}$ ,  $P^{(1)}$  and  $P^{(2)}$ .

tually, the virtual atom acts as an additional message proxy between nodes in the molecular graph.

The sequence  $(a_0, a_1, \dots, a_n)$  is embedded into a corresponding sequence of latent node representations  $(\hat{a}_0, \hat{a}_1, \dots, \hat{a}_n) \in \mathbb{R}^d$ , where each  $\hat{a}_i$  is a learnable vector associated with the atom type.

Additionally, let  $z_i \in \mathbb{R}^d$  be a learnable embedding that depends on the number of bonds formed by the  $i$ -th atom. The augmented sequence  $(\hat{a}_0, \hat{a}_1 + z_1, \dots, \hat{a}_n + z_n)$  is then passed through a stack of transformer layers using ReZero normalization (Bachlechner et al., 2021). Importantly, to preserve the permutation equivariance of the network (i.e., the order of the atoms does not matter), no positional encoding is applied.

To incorporate bonding information within the transformer layers, let  $(A_{ij})_{0 \leq i, j \leq n} \in \mathbb{R}^{(n+1) \times (n+1)}$  be the computed self-attention matrix in a layer (for any attention head) corresponding to the input sequence  $(a_0, a_1, \dots, a_n)$ . As in Graphormer (Ying et al., 2021), and similar to the Molecule Attention Transformer (Maziarka et al., 2019), we augment the attention matrix  $A$  by introducing bond-specific information. This is done by adding a learnable bias to the attention scores before applying the softmax operation. Specifically, for  $0 \leq i, j \leq n$ , the attention score  $A_{ij}$  between the  $i$ -th and  $j$ -th sequence elements is modified as follows:

$$A_{ij} \leftarrow A_{ij} + b_{ij}, \quad (3)$$

where  $b_{ij} \in \mathbb{R}$  is a learnable scalar that only depends on the bond order  $B_{ij}$  for  $i, j > 0$  (and not on the indices  $i, j$ ). In particular, for the special bonds involving the virtual atom (i.e., if  $i = 0$  or  $j = 0$ ),  $b_{ij} = b$  is a learnable scalar shared

across all atoms. We note that  $b_{ij}$  for each bond order is learned independently across layers and attention heads.

**Action distribution** The stack of transformer layers produces a transformed sequence of node embeddings  $(e_0, e_1, \dots, e_n)$ , where each  $e_i \in \mathbb{R}^d$  corresponds to the  $i$ -th atom  $a_i$  in the original sequence. This sequence is used to predict three distributions,  $P^{(0)}$ ,  $P^{(1)}$ ,  $P^{(2)}$ , which together factorize the full distribution over possible next actions.

Informally,  $P^{(0)}$  represents a distribution over whether to terminate the synthesis, add a new atom, or increase the bond order between two existing atoms. The distribution  $P^{(1)}$  specifies which atom to select, either as the atom to bond a newly added atom to, or as the first atom of a pair for increasing bond order. Finally,  $P^{(2)}$  is used in the case of bond increase to specify the second atom in the pair. Formally, the unnormalized log-probabilities (logits) for these distributions are obtained as follows:

- $P^{(0)}$ : We compute the logits for  $P^{(0)} = (p_0^{(0)}, p_1^{(0)}, \dots, p_k^{(0)}, p_{k+1}^{(0)})$  by projecting the vector  $e_0$  using a linear layer  $g_0: \mathbb{R}^d \rightarrow \mathbb{R}^{k+2}$ . Here,  $p_0^{(0)}$  is the probability of choosing the action DONTCHANGE. For  $1 \leq j \leq k$ ,  $p_j$  represents the probability of adding an atom of type  $\Sigma_k$  (i.e., ADDATOM( $j, \cdot$ ) without specifying the bonding atom yet). Lastly,  $p_{k+1}^{(0)}$  is the probability of increasing the bond between two atoms (INCBOND( $\cdot, \cdot$ )) without specifying the atom pair.
- $P^{(1)}$ : To obtain  $P^{(1)} = (p_1^{(1)}, \dots, p_n^{(1)})$ , we apply a linear layer  $g_1: \mathbb{R}^d \rightarrow \mathbb{R}$  independently to each

$e_1, \dots, e_n$ . Then,  $p_j^{(1)}$  represents the probability of selecting the  $j$ -th atom to bond to in  $\text{ADDATOM}(\cdot, \cdot)$ , or as the first atom in  $\text{INCBOND}(\cdot, \cdot)$ .

- $P^{(2)}$ : Similarly, for  $P^{(2)} = (p_1^{(2)}, \dots, p_n^{(2)})$ , we apply another linear layer  $g_2: \mathbb{R}^d \rightarrow \mathbb{R}$  to compute the logits for the probability  $p_l^{(2)}$ , representing the likelihood of selecting the  $l$ -th atom as the second atom in  $\text{INCBOND}$ .

In practice, during inference, we use  $P^{(0)}$  and  $P^{(1)}$  directly to choose the first atom for both  $\text{ADDATOM}$  and  $\text{INCBOND}$ , and discard  $P^{(2)}$ . If  $\text{INCBOND}$  has been selected from  $P^{(0)}$ , we reprocess the molecule through the network, marking the atom chosen from  $P^{(1)}$  by adding a distinct learnable embedding to its corresponding sequence element. In this second pass, we use only  $P^{(2)}$  to select the second atom for  $\text{INCBOND}$ .

This multi-step action prediction allows us to easily mask actions (i.e., setting their probability to zero in the policy) that would lead to invalid molecules. While checking for actions that would violate constraints adds a small amount of computational overhead, it has a significant benefit: invalid molecules can be immediately disregarded, preventing the network from wasting resources on infeasible designs. Masking invalid actions not only reduces the search space but also speeds up training by avoiding the need for the model to learn through trial and error how to avoid invalid molecules.

### 3. Results and Discussion

First, we outline our design tasks, including the objective functions and property prediction methods. Next, we describe the experimental setup common to all methods and outline the specific setup and hyperparameters for our method, followed by a brief overview of the methods used for comparison. We then present preliminary baseline objectives obtained from screening a list of available molecules and discuss our results in relation to those of the other methods.

#### 3.1. Example solvent design tasks

**Objectives** We aim to design solvents for two-phase aqueous-organic systems used in liquid-liquid extraction. Our focus is on two examples motivated by biotechnology, where products are typically produced in an aqueous solution using microorganisms or enzymes. In such processes, products are to be extracted using the organic solvents we aim to design. We assume a spatially uniform temperature of 298 K in both examples.

The first task focuses on the separation of isobutanol (IBA) from water, a common liquid-liquid extraction process. The

chosen solvent should be largely immiscible with water (i.e., low solubility exhibited for both the solvent in water and water in the solvent) and possess high affinity for IBA. As is common practice in chemical engineering, we use the partition coefficient  $P_{\text{IBA}}^\infty$  at small mole fractions of IBA in both phases  $x_{\text{IBA}}$ :

$$P_{\text{IBA}}^\infty = \lim_{x_{\text{IBA}}^{\text{W}} \rightarrow 0} \frac{x_{\text{IBA}}^{\text{S}}}{x_{\text{IBA}}^{\text{W}}} \quad (4)$$

where  $x_{\text{IBA}}^{\text{W}}$  and  $x_{\text{IBA}}^{\text{S}}$  are the mole fractions of IBA in water (W) and the solvent (S), respectively. This coefficient serves as a simple yet effective measure of the relative affinity of the solvent compared to water. Assuming low mutual solubility between the solvent and water,  $P_{\text{IBA}}^\infty$  can be well approximated by the ratio of IBA’s activity coefficients at infinite dilution,  $\gamma_{\text{IBA,W}}^\infty$  and  $\gamma_{\text{IBA,S}}^\infty$ , in water and solvent, respectively:

$$P_{\text{IBA}}^\infty = \frac{\gamma_{\text{IBA,W}}^\infty}{\gamma_{\text{IBA,S}}^\infty}. \quad (5)$$

To ensure the formation of two phases, i.e., a miscibility gap between the solvent and water, we use the following constraint:

$$\gamma_{\text{S,W}}^\infty \cdot \gamma_{\text{W,S}}^\infty > \exp(4). \quad (6)$$

This constraint guarantees a phase split between the water and solvent, assuming that the activity coefficient profiles follow the two-parameter Margules  $g^E$  model (Wisniak, 1983). Although the activity coefficients of all conceivable solvent/water mixtures will not necessarily follow this model, the constraint still serves as a useful indicator for miscibility gaps.

The partition coefficient and the miscibility gap constraint are then combined to form the following scalar objective function:

$$\max \frac{1}{\gamma_{\text{IBA,S}}^\infty} + (\tanh(\gamma_{\text{S,W}}^\infty \cdot \gamma_{\text{W,S}}^\infty - \exp(4)) - 1) \cdot 10. \quad (7)$$

Hereby, the solvent-independent constant  $\gamma_{\text{IBA,W}}^\infty$  is omitted.

Our second task centers on an extraction process presented by Peters et al. (2008), who carried out a solvent screening using COSMO-RS as a property predictor. Here, an enzymatic reaction in aqueous medium converts 3,5-dimethoxybenzaldehyde (DMBA) molecules to (R)-3,3',5,5'-tetramethoxybenzoin (TMB). The task is to find an organic solvent that forms a two-phase system with water. Similar to the IBA task, an optimal solvent should have a high affinity for the product TMB, enabling it to pull TMB out of the aqueous phase. At the same time, however, the solvent should have a low affinity for the educt DMBA. Designing

a suitable solvent for this task is extremely challenging because DMBA and TMB possess similar chemical structures and polarities.

Again assuming small concentrations of DMBA and TMB as well as low mutual solubility between the solvent and water, we define the following partition coefficients similarly to our IBA task:

$$\begin{aligned} P_{\text{DMBA}}^{\infty} &= \frac{\gamma_{\text{DMBA,W}}^{\infty}}{\gamma_{\text{DMBA,S}}^{\infty}} \\ P_{\text{TMB}}^{\infty} &= \frac{\gamma_{\text{TMB,W}}^{\infty}}{\gamma_{\text{TMB,S}}^{\infty}}. \end{aligned} \quad (8)$$

Following Peters et al. (2008), we maximize the ratio  $P_{\text{TMB}}^{\infty}/P_{\text{DMBA}}^{\infty}$ , while additionally enforcing the miscibility gap constraint from Equation 6 leading to the following scalar objective:

$$\max \frac{\gamma_{\text{TMB,S}}^{\infty}}{\gamma_{\text{DMBA,S}}^{\infty}} + (\tanh(\gamma_{\text{S,W}}^{\infty} \cdot \gamma_{\text{W,S}}^{\infty} - \exp(4)) - 1) \cdot 10. \quad (9)$$

Hereby, we again omitted the constants  $\gamma_{\text{TMB,W}}^{\infty}$  and  $\gamma_{\text{DMBA,W}}^{\infty}$ .

**Property prediction** To obtain activity coefficients at infinite dilution, we use a state-of-the-art graph neural network (GNN) (Gilmer et al., 2017; Reiser et al., 2022; Rittig et al., 2023c). Specifically, we employ the Gibbs-Helmholtz (GH-) GNN that was developed by Medina et al. (2023) for predicting activity coefficients at infinite dilution of binary mixtures at varying temperature. The GH-GNN takes the molecular graphs of the two molecules within a binary mixture and the temperature as inputs. First, structural information from the individual molecular graphs and molecular (self-)interactions based on a mixture graph are encoded into a vector representation, the mixture fingerprint. Based on the mixture fingerprint, a multilayer perceptron (MLP) then predicts the parameters of the Gibbs-Helmholtz relationship so that infinite dilution activity coefficients can be predicted with temperature. The GH-GNN is trained in a structure-to-property manner, i.e., it directly learns activity coefficients at infinite dilution as a function of the molecular graphs. A large data set of experimental activity coefficients at infinite dilution from the DECHEMA Chemistry Data Series (Gmehling et al., 2008) was used for training. For further details on the GH-GNN architecture, we refer to Medina et al. (2023).

We note that many GNN models and other ML models such as transformers have been developed for activity coefficient prediction (Rittig et al., 2023a; Winter et al., 2022; Damay et al., 2021), also considering the composition-dependency and thermodynamic consistency (Rittig et al., 2023b; Winter et al., 2023; Rittig & Mitsos, 2024; Specht et al., 2024).

We here chose the GH-GNN as it is specialized for activity coefficients at infinite dilution and was trained on a much larger experimental database than the other models, thus covering a larger chemical space (Medina et al., 2023), which is desirable for molecular design. This model has shown high prediction accuracy, outperforming well-established methods for predicting activity coefficients at infinite dilution such as UNIFAC (Fredenslund et al., 1975) or COSMO-RS (Klamt et al., 2010), cf. (Medina et al., 2023). Future work could investigate further additional activity coefficient models or directly predicting partition coefficients with ML (Zamora et al., 2023; Nevolianis et al., 2024).

### 3.2. General computational setup

To ensure comparability across methods in the design task, we restrict the set of available atoms to carbon, nitrogen, and oxygen (alphabet  $\Sigma = (\text{C}, \text{N}, \text{O})$ ). In the solvent design tasks we consider, molecules are evaluated using objective functions based on a surrogate model for predicting activity coefficients (see Section 3.1). To avoid potential exploitation of the surrogate model by constructing large molecules that are beyond the size of typically used solvents and thus likely to be different from the molecules used to train the surrogate model, we constrain the design to molecules of a moderate size, with a maximum of 25 atoms. The runtime of a method can vary significantly due to differences in implementation or available hardware. One approach to align computational resources is to limit the number of calls to the objective function (Gao et al., 2022). While this method is useful for comparing sample efficiency, it provides limited insight into the overall efficiency of a method when objective function evaluations are relatively inexpensive. Given the efficiency of the surrogate model, objective function evaluations can be parallelized and run in batches very quickly. Therefore, we take a practical approach to align computational resources: each design run of a method is allocated a time budget of eight wall-clock hours on identical hardware, utilizing a single NVIDIA H100 GPU with 80 GB of memory.

### 3.3. Our method: GraphXForm

**Network hyperparameters** For all our experiments, we set the dimension of the latent space  $\mathbb{R}^d$  to  $d = 128$  (see Section 2.3). The network consists of eight transformer layers with ReZero normalization, each with eight heads in the multi-head attention, and a feed-forward dimension of 512.

**Pretraining** While it is possible for the agent to learn without any prior knowledge of existing compounds, we pretrain the network on known molecules using SMILES strings from the ChEMBL database (Davies et al., 2015). We filtered the database to ensure the molecules contain



only atoms within the alphabet  $\Sigma$ , yielding approximately 370,000 molecules. Each SMILES string is then converted into an action sequence in our graph formulation. Since this conversion is not unique, we arbitrarily select one possible action sequence. The resulting sequences are used to train the model in a self-supervised way, predicting the next action given the previous actions, as outlined in lines 12-14 in Algorithm 1. Training is conducted with a batch size of 128, over a total of 2.5 million batches.

Petraining the network on existing molecules establishes a prior that captures the characteristics of real molecules, which is crucial for most generative methods such as REINVENT (Olivecrona et al., 2017; Xu et al., 2024) or JT-VAE (Jin et al., 2018).

**Fine-tuning** Given an objective function  $f: \mathcal{M}' \rightarrow \mathbb{R} \cup \{-\infty\}$ , we fine-tune the pretrained policy network using the learning algorithm described in Section 2.2. Unless stated otherwise, we initialize the molecule  $m_0$  as a single carbon atom. We set  $s = 500$  as the number of top molecules to retain throughout training. In each epoch, we sample between  $q_{\min} = 10 \cdot 1024$  and maximum of  $q_{\max} = 50 \cdot 1024$  unique action sequences. At the end of each epoch, we train the network on 20 batches of size 64, sampled uniformly from the top 500 molecules. We intentionally keep the number of training batches per epoch relatively low for the network’s size to prevent premature overfitting in all considered cases. However, we observe that in most runs, training on more batches does not adversely affect performance and can actually increase the speed of convergence.

### 3.4. Benchmark methods

We compare our proposed approach with four diverse molecular design methods: Graph GA (Jensen, 2019) (a genetic algorithm (GA) applied to molecular graphs), REINVENT-Transformer (Xu et al., 2024) (a transformer model that generates SMILES strings), Junction Tree VAE (Jin et al., 2018) combined with a GA for optimization in latent molecular space, and STONED (Nigam et al., 2021) (which performs string mutations on the SELFIES (Krenn et al., 2020) representation). For benchmarking, we use the source code provided by Gao et al. (2022). Although these methods employ different paradigms, we apply the same objective function across all methods to guide the design process.

**Graph GA and STONED** Graph GA (Jensen, 2019) uses a GA that directly operates on the molecular graph by mutating atoms and fragments, using crossover rules derived from graph matching. It is a strong non-learning method that has been shown to outperform several SMILES-based learning approaches (Jensen, 2019; Gao et al., 2022). In contrast, STONED (Nigam et al., 2021) employs a GA that operates on the string level and manipulates tokens within

the SELFIES molecular representation (Krenn et al., 2020).

**REINVENT-Transformer** REINVENT-Transformer (Xu et al., 2024) is a recent state-of-the-art method for designing molecules by synthesizing SMILES strings in an autoregressive way. The approach involves a transformer network that is pretrained in a self-supervised manner on known molecules and then fine-tuned with reinforcement learning using a variant of the REINFORCE algorithm (Williams, 1992). REINVENT-Transformer is similar to GraphXForm in that both rely on pretrained transformers and generate molecules autoregressively. However, REINVENT-Transformer constructs molecules in a language-like manner by building a string token by token from an allowed vocabulary, whereas GraphXForm operates directly on the molecular graph by adding atoms and bonds.

This direct manipulation of the molecular graph allows GraphXForm to guarantee the design of feasible molecules by construction, whereas REINVENT-Transformer must learn the SMILES grammar to avoid invalid structures. Additionally, our approach can start from arbitrary structures, unlike the left-to-right string construction in REINVENT-Transformer, making it straightforward to encode specific constraints to limit the search space. For a fair comparison, we pretrain the policy for REINVENT-Transformer using the same dataset as GraphXForm.

**Junction Tree VAE** We further use variational autoencoders (VAEs) that have been widely used as a generative model in ML-guided molecular design, cf. overviews in Refs. (Sanchez-Lengeling & Aspuru-Guzik, 2018; Bilodeau et al., 2022; Anstine & Isayev, 2023). VAEs use an encoder-decoder structure: The encoder maps molecules to a continuous vector representation, referred to as latent space, from which the decoder reconstructs these molecules. The molecular latent space can facilitate exploration of the molecular space. That is, different optimization strategies can be employed to discover points in the latent space that correspond to promising novel molecules. These strategies include random sampling, Bayesian optimization, and GAs (Sanchez-Lengeling & Aspuru-Guzik, 2018; Rittig et al., 2023d; Anstine & Isayev, 2023).

We herein use the Junction Tree VAE (JT-VAE) (Jin et al., 2018) in combination with GAs. The JT-VAE operates on molecular graphs and their non-cyclic abstractions (junction trees), and has shown a high rate of decoding vectors from its latent space to chemically valid molecules. For the solvent design task, we only consider molecules that conform to the alphabet  $\Sigma$ . We therefore train JT-VAE on a subset of the QM9 data set, which consists of about 128,000 molecules containing at most nine heavy atoms. We use GAs to optimize within the JT-VAE latent space because they enable exploring a large number of latent vectors, hence molecules,

due to the linear scaling with the number of sampling points.

### 3.5. Design results

The goal for all methods is to find suitable solvents with respect to the two objectives from Equations 7 and 9 for the two example problems, using the general setup outlined in Section 3.2.

**Screening list** To contextualize the results of all methods, we selected all 6,098 compounds from the COSMObase 2020 database that conform to the alphabet  $\Sigma$ . We calculated the objective functions for those compounds that also meet the miscibility gap requirements, cf. (6). The top three compounds based on their objective values are shown in the first column in Figures 3 and 4. For the IBA task, the best molecule in this list achieves an objective value of 5.57, while for the TMB/DMBA task, the highest objective value is 3.03.

**Model results** Table 1 compares the performance of the different molecular design methods for the two solvent design tasks. We report the objective value of the best molecule found by each method, as well as the average objective values of the top 20 molecules. We also present results averaged over multiple runs with different random seeds, providing insight into the robustness of each method. Additionally, Figures 3 and 4 display the structural formulas of the top three molecules identified by each method.

In the IBA task, GraphXForm, REINVENT-Transformer, and Graph GA all identified the same best molecule, which has an objective value of 8.87. However, GraphXForm consistently found this molecule in every run, highlighting its stability. For example, in contrast, while Graph GA achieved the same average value for the top 20 molecules, its mean best objective was only 7.13.

For the more challenging TMB/DMBA task, GraphXForm significantly outperforms all others across every metric. Notably, Graph GA performs better overall than the recent REINVENT-Transformer, likely due to REINVENT-Transformer’s sensitivity to initialization during RL fine-tuning. This is also reflected in its relatively high standard deviation compared to the other methods.

Interestingly, the JT-VAE and STONED methods identified molecules with significantly lower objective values for the TMB/DMBA task when compared to other methods, with maximum values of approximately 2.16 and 2.39, respectively. However, their results for the IBA task (6.85 and 7.53) were closer to those of the other methods. We attribute this discrepancy to the nature of the tasks: The TMB/DMBA task is inherently more challenging and requires larger, more complex molecules, while the best-performing molecules in the IBA task were smaller. As JT-VAE was trained only

on molecules with up to nine heavy atoms, its ability to explore larger molecules seems limited. Similarly, STONED struggled to effectively explore larger molecular structures.

In summary, GraphXForm demonstrates highly promising results in both solvent design tasks, outperforming state-of-the-art molecular design methods in terms of identifying the best candidates and ensuring robustness in the design process. In the following sections, we further explore the flexibility of GraphXForm by imposing structural constraints on the designed molecules and starting the design process from initial molecular structures.

### 3.6. Including structural constraints in molecular design

In addition to optimizing an objective, such as a physical property, it is often desirable to enforce specific structural characteristics in the generated molecular candidates. These structural constraints can include limitations on ring size or specific bonding patterns between atom types, which can improve chemical feasibility, such as enhancing synthesizability and stability or reducing toxic moieties. For instance, in the TMB/DMBA task, although the top molecules generated by GraphXForm exhibit high objective values, they possess several characteristics that pose challenges for solvent design. Notably, the presence of single nitrogen-nitrogen bonds often leads to instability (hyd, 2024), resulting in reactive compounds that are unsuitable for liquid-liquid extraction. Additionally, the existence of a nine-member ring could pose significant challenges to the solvent’s synthesizability (Steinborn et al., 2023).

As noted in Section 2.1, string-based molecular design methods cannot directly enforce such structural constraints. Typically, this is managed by assigning a very low objective value to molecules that violate these constraints. In contrast, by operating directly on the molecular graph, GraphXForm allows us to restrict the search space for many constraints by simply masking actions that would lead to constraint-violating molecules. To examine how structural constraints affect the performance of GraphXForm in finding molecules with high objective values, we impose the following constraints: We limit the ring size to a maximum of six atoms and disallow any bonds between two oxygen atoms as well as single bonds between two nitrogen atoms. We note that these constraints of course do not cover all possibilities for maintaining synthetic accessibility and chemical stability; instead, they serve as examples to illustrate the capabilities of GraphXForm.

For the IBA task, the best molecule identified in Table 1 with objective value of 8.87 contains multiple nitrogen-nitrogen single bonds. We therefore rerun the design task with the additional structural constraints. The top three molecules designed by GraphXForm in these runs are shown in the top row of Figure 5. With constraints, we achieve

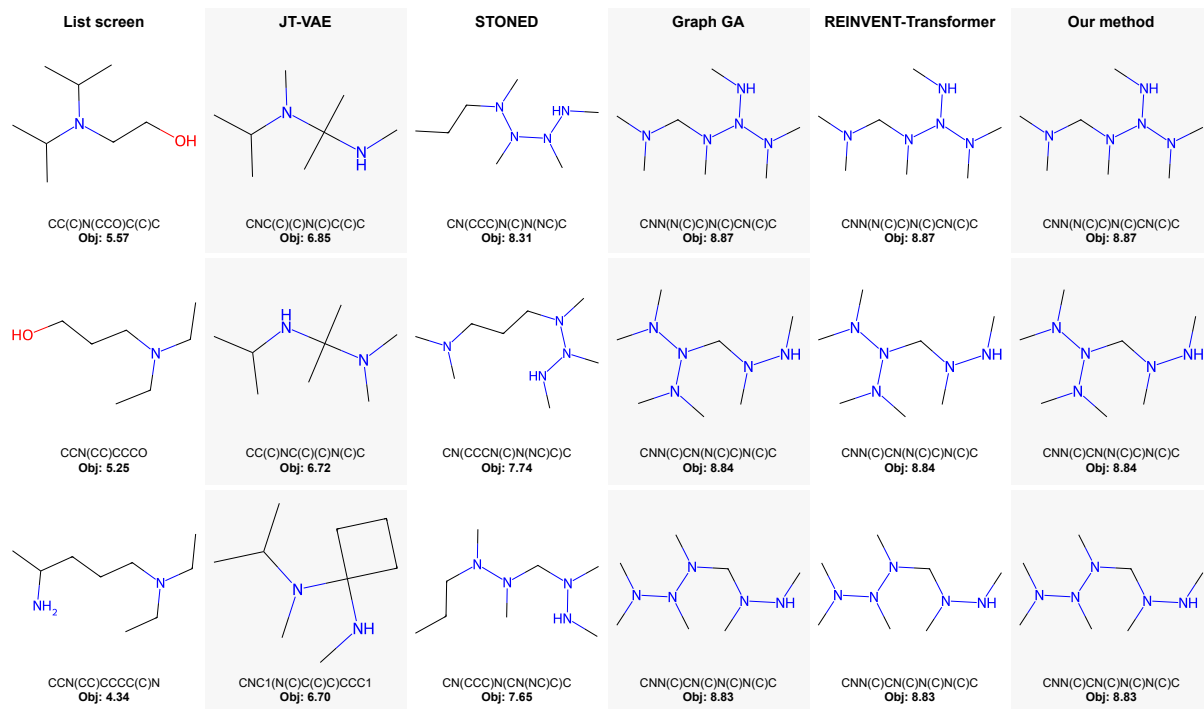


Figure 3. **IBA task**: Top three molecules (with their corresponding SMILES string and objective value) identified by each method across all runs.

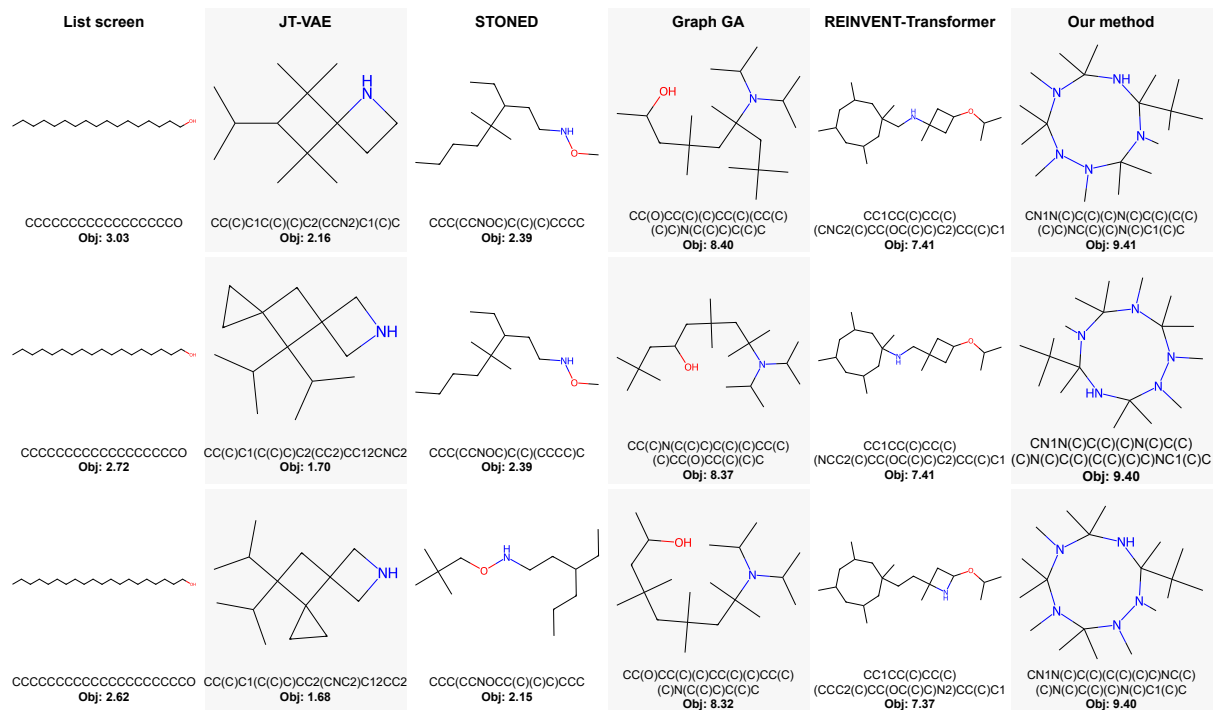


Figure 4. **TMB/DMBA task**: Top three molecules (with their corresponding SMILES string and objective value) identified by each method across all runs.

Table 1. Performance of different molecular design methods for the two example tasks. Each method is run across three different random seeds, with a time budget of 8 hours. We report the objective function evaluation of the best molecule found over all runs (‘max best’), best averaged over all the three runs  $\pm$  standard deviation (‘mean best’), the average of the top 20 molecules of the best run (‘max top 20’), and the mean of the top 20 over all three runs  $\pm$  standard deviation (‘mean top 20’).

Method	IBA (cf. (7))				TMB/DMBA (cf. (9))			
	max best	mean best	max top 20	mean top 20	max best	mean best	max top 20	mean top 20
JT-VAE (Jin et al., 2018)	6.85	6.41 $\pm$ 0.66	6.04	5.68 $\pm$ 0.57	2.16	1.56 $\pm$ 0.54	1.44	1.20 $\pm$ 0.23
STONED (Nigam et al., 2021)	8.31	7.42 $\pm$ 0.94	6.72	6.28 $\pm$ 0.41	2.39	1.68 $\pm$ 0.65	1.91	1.45 $\pm$ 0.49
Graph GA (Jensen, 2019)	<b>8.87</b>	7.13 $\pm$ 3.01	<b>8.67</b>	6.80 $\pm$ 3.22	8.40	8.14 $\pm$ 0.27	8.07	7.95 $\pm$ 0.32
REINVENT-Transformer (Xu et al., 2024)	<b>8.87</b>	8.32 $\pm$ 0.52	8.66	8.09 $\pm$ 0.45	7.41	6.52 $\pm$ 1.17	7.22	6.42 $\pm$ 0.96
<b>GraphXForm (ours)</b>	<b>8.87</b>	<b>8.87 <math>\pm</math> 0.00</b>	<b>8.67</b>	<b>8.67 <math>\pm</math> 0.00</b>	<b>9.41</b>	<b>9.33 <math>\pm</math> 0.12</b>	<b>9.23</b>	<b>9.14 <math>\pm</math> 0.11</b>

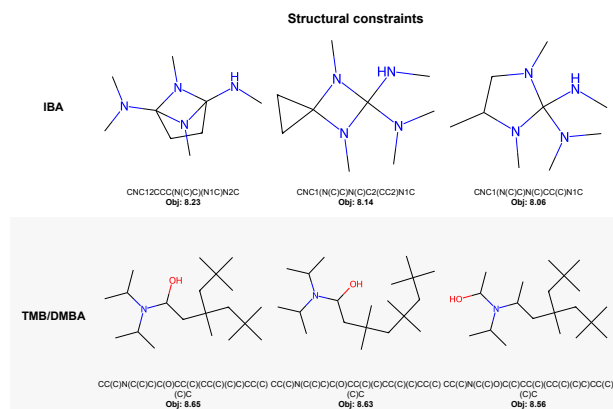


Figure 5. Top three molecules designed by GraphXForm where: ring size is limited to a maximum of six atoms, any bond between oxygen atoms is disallowed, and single bonds between nitrogen atoms are disallowed.

a ‘mean best’ value of  $8.23 \pm 0.00$  and a ‘mean top 20’ value  $7.98 \pm 0.02$ , which are only slightly lower than the values obtained without structural constraints. We also repeated these constrained design runs with REINVENT-Transformer, given its conceptual similarity to GraphXForm. However, REINVENT-Transformer only reached a ‘mean best’ value of  $7.03 \pm 1.14$ , with its overall best molecule having an objective value of 7.87.

The top three molecules identified by GraphXForm with the structural constraints for the TMB/DMBA task are shown in the bottom row of Figure 5. Under these constraints, GraphXForm achieves a ‘mean best’ value of  $8.65 \pm 0.00$  and a ‘mean top 20’ value of  $8.42 \pm 0.03$ . Notably, these results remain superior to those of the other methods that do not impose structural constraints listed in Table 1.

This further demonstrates GraphXForm’s flexibility and its ability to consistently design promising molecules.

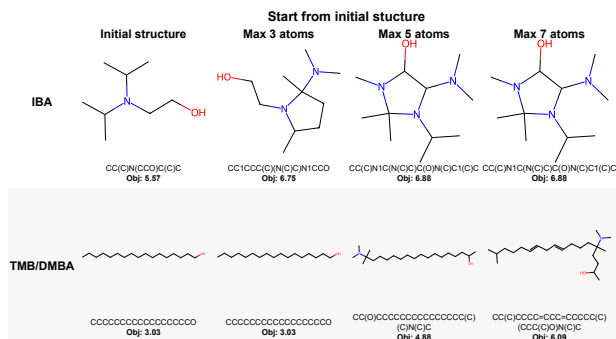


Figure 6. Best molecule designed by GraphXForm when adding a maximum of 3, 5, and 7 atoms to a specific initial structure. We note that increasing the order of a bond within the initial structure is allowed. For TMB/DMBA, we also enforce that the designed molecule stays an alcohol.

### 3.7. Starting molecule design from initial structures

One advantage of GraphXForm, which is not feasible when constructing SMILES strings via next-token prediction due to the linear construction, is the ability to start the molecule design process from a predefined structure. This feature is particularly useful when a known candidate, potentially in practical use, possesses desirable properties but could benefit from slight modifications to improve the objective function. To demonstrate this, we consider the IBA task and begin with the best molecule from COSMObase 2020, which has an objective value of 5.57 (see Figure 4). We conduct three individual experiment runs, allowing GraphXForm to add up to 3, 5, and 7 atoms to the initial structure (and alter bond orders as needed). We also maintain the structural constraints outlined in Section 3.6. The original molecule, along with the best molecule from each of the three runs, is shown in the first row of Figure 6. In all cases, the designed molecules exhibit improvements in the objective value.

We repeat a similar experiment for the TMB/DMBA task. During the list screening, we observed that the top three structures were all long-chain alcohols. However, long-

chain alcohols tend to have melting points above room temperature, making them unsuitable as solvents for the processes under consideration. The melting point can be lowered by adding branches and increasing bond orders. Thus, we initiate three runs starting from the best molecule identified in the list screening, allowing the addition of up to 3, 5, or 7 atoms, respectively. Additionally, we constrain the design process to ensure the resulting molecule remains an alcohol by preventing any actions from being taken on the hydroxy group (one oxygen bonded to one hydrogen). The results are shown in the second row of Figure 6. While no better molecule is found when adding only up to 3 atoms, a notable improvement occurs when allowing to add 5 or 7 atoms.

This approach provides a powerful tool for situations where it is preferable not to start the design process from scratch but to make targeted modifications to existing molecules.

We note that allowing the agent to remove atoms or bonds would not provide any benefit when starting the design from scratch, i.e., from a single atom. In fact, it would introduce additional redundancies into the search space. However, in the discussed scenarios where the design begins with an existing molecule, enabling the agent to remove atoms or bonds could in fact offer an advantage, as it allows for greater flexibility and deviations from the initial structure. We leave the exploration of this possibility for future work.

## Conclusion

We presented GraphXForm, a method for molecular design that follows the successful paradigm of self-supervised pre-training followed by (RL-based) fine-tuning, but operates directly on molecular graphs. By doing so, we addressed challenges faced by string-based methods, such as chemical validity or accommodating structural constraints. We introduced a technique derived from self-improvement learning to stably fine-tune a deep graph-transformer model with eight layers. On two solvent design tasks, we showed that GraphXForm can outperform state-of-the-art molecule design techniques. Additionally, our approach can flexibly adhere to specified structural constraints, such as bond types and functional groups, and can adaptively start the design process from existing molecular structures.

Looking ahead, several promising avenues for future development exist. First, we could expand GraphXForm to include more atoms and ionization states, as well as pretrain the network on much larger databases. We note that these features can already be integrated within our current framework; however, we restricted the set of possible atoms to ensure comparability between our and other methods. We could further evaluate GraphXForm on additional solvent design tasks, as well as more extensively researched drug

design tasks.

We also aim to incorporate more constraints to ensure the suitability of solvents for liquid-liquid separation processes, recognizing that numerous factors – such as boiling and melting points – are critical to a solvent’s effectiveness. This, however, will depend on the availability of reliable property predictors.

Finally, since many structural constraints (e.g., presence of certain atoms, bonds, or formal groups) on the molecular graph can be flexibly formulated and implemented in a general manner within the current framework, we envision integrating GraphXForm with large language models to create a user-friendly design interface. This would allow researchers to formulate constraints in natural language, which would then be translated into the appropriate configuration for the model.

## Author contributions

J.P.: Conceptualization; Methodology - Concept and implementation of environment, network architecture, learning algorithm, adaptation of benchmark methods; Analysis; Validation; Visualization; Writing - Original Draft. J.G.R.: Conceptualization; Methodology - Concept and implementation of objective functions and surrogate models, adaptation of benchmark methods; Analysis; Validation; Writing - Original Draft. A.B.W.: Conceptualization; Methodology - Concept and implementation of environment and objective functions, adaptation of benchmark methods; Analysis; Validation; Visualization; Writing - Original Draft. M.G.: Resources; Funding acquisition; Writing - Review & Editing. J.B.: Conceptualization; Resources; Supervision; Project administration; Funding acquisition; Writing - Review & Editing. A.M.: Conceptualization; Resources; Supervision; Project administration; Funding acquisition; Writing - Review & Editing. D.G.G.: Conceptualization; Resources; Supervision; Project administration; Funding acquisition; Writing - Review & Editing.

## Data availability

All our code and data for pretraining and fine-tuning GraphXForm is available at <https://github.com/grimmlab/graphxform>.

## Acknowledgements

This project was funded by the Deutsche Forschungsgemeinschaft (DFG, German Research Foundation) – 466417970 and 466387255 – within the Priority Programme “SPP 2331: Machine Learning in Chemical Engineering”. This work was performed as part of the Helmholtz School for Data Science in Life, Earth and Energy (HDS-LEE). Simula-

tions were performed with computing resources granted by RWTH Aachen University under project “thes1232”. The authors gratefully acknowledge the Competence Center for Digital Agriculture (KoDA) at the University of Applied Sciences Weihenstephan-Triesdorf for providing additional computational resources.

## References

- National center for biotechnology information. pubchem compound database, 2024. URL <https://pubchem.ncbi.nlm.nih.gov/>.
- Anstine, D. M. and Isayev, O. Generative models as an emerging paradigm in the chemical sciences. *Journal of the American Chemical Society*, 145(16):8736–8750, 2023.
- Bachlechner, T., Majumder, B. P., Mao, H., Cottrell, G., and McAuley, J. Rezero is all you need: Fast convergence at large depth. In *Uncertainty in Artificial Intelligence*, pp. 1352–1361. PMLR, 2021.
- Bilodeau, C., Jin, W., Jaakkola, T., Barzilay, R., and Jensen, K. F. Generative models for molecular discovery: Recent advances and challenges. *Wiley Interdisciplinary Reviews: Computational Molecular Science*, 12(5):e1608, 2022.
- Bjerrum, E. J. and Threlfall, R. Molecular generation with recurrent neural networks (rnns). *arXiv preprint arXiv:1705.04612*, 2017.
- Cheng, A. H., Cai, A., Miret, S., Malkomes, G., Phielipp, M., and Aspuru-Guzik, A. Group selfies: a robust fragment-based molecular string representation. *Digital Discovery*, 2(3):748–758, 2023.
- Corsini, A., Porrello, A., Calderara, S., and Dell’Amico, M. Self-labeling the job shop scheduling problem. *arXiv preprint arXiv:2401.11849*, 2024.
- Dai, H., Tian, Y., Dai, B., Skiena, S., and Song, L. Syntax-directed variational autoencoder for structured data. *arXiv preprint arXiv:1802.08786*, 2018.
- Damay, J., Jirasek, F., Kloft, M., Bortz, M., and Hasse, H. Predicting activity coefficients at infinite dilution for varying temperatures by matrix completion. *Industrial & Engineering Chemistry Research*, 60(40):14564–14578, 2021. ISSN 0888-5885. doi: 10.1021/acs.iecr.1c02039.
- Davies, M., Nowotka, M., Papadatos, G., Dedman, N., Gaulton, A., Atkinson, F., Bellis, L., and Overington, J. P. ChEMBL web services: streamlining access to drug discovery data and utilities. *Nucleic acids research*, 43(W1):W612–W620, 2015.
- De Cao, N. and Kipf, T. Molgan: An implicit generative model for small molecular graphs. *arXiv preprint arXiv:1805.11973*, 2018.
- Devlin, J. Bert: Pre-training of deep bidirectional transformers for language understanding. *arXiv preprint arXiv:1810.04805*, 2018.
- Fredenslund, A., Jones, R. L., and Prausnitz, J. M. Group-contribution estimation of activity coefficients in nonideal liquid mixtures. *AIChE Journal*, 21(6):1086–1099, 1975. ISSN 00011541. doi: 10.1002/aic.690210607.
- Fu, T., Gao, W., Coley, C., and Sun, J. Reinforced genetic algorithm for structure-based drug design. *Advances in Neural Information Processing Systems*, 35:12325–12338, 2022.
- Gao, W., Fu, T., Sun, J., and Coley, C. Sample efficiency matters: a benchmark for practical molecular optimization. *Advances in neural information processing systems*, 35:21342–21357, 2022.
- Gilmer, J., Schoenholz, S. S., Riley, P. F., Vinyals, O., and Dahl, G. E. Neural message passing for quantum chemistry. *34th International Conference on Machine Learning, ICML 2017*, 3:2053–2070, 2017.
- Gmehling, J., Tiegs, D., Medina, A., Soares, M., Bastos, J., Alessi, P., Kikic, I., Schiller, M., and Menke, J. Dechema chemistry data series, volume ix activity coefficients at infinite dilution. *DECHEMA Chemistry Data Series*, 9, 2008.
- Gómez-Bombarelli, R., Wei, J. N., Duvenaud, D., Hernández-Lobato, J. M., Sánchez-Lengeling, B., Sheberla, D., Aguilera-Iparraguirre, J., Hirzel, T. D., Adams, R. P., and Aspuru-Guzik, A. Automatic chemical design using a data-driven continuous representation of molecules. *ACS central science*, 4(2):268–276, 2018.
- Gupta, A., Müller, A. T., Huisman, B. J., Fuchs, J. A., Schneider, P., and Schneider, G. Generative recurrent networks for de novo drug design. *Molecular informatics*, 37(1-2):1700111, 2018.
- Henderson, P., Islam, R., Bachman, P., Pineau, J., Precup, D., and Meger, D. Deep reinforcement learning that matters. In *Proceedings of the AAAI conference on artificial intelligence*, volume 32, 2018.
- Huang, J., Gu, S. S., Hou, L., Wu, Y., Wang, X., Yu, H., and Han, J. Large language models can self-improve. In *The 2023 Conference on Empirical Methods in Natural Language Processing*, 2023. URL <https://openreview.net/forum?id=uuUQraD4XX>.

- Jensen, J. H. A graph-based genetic algorithm and generative model/monte carlo tree search for the exploration of chemical space. *Chemical science*, 10(12):3567–3572, 2019.
- Jiang, S., Dieng, A. B., and Webb, M. A. Property-guided generation of complex polymer topologies using variational autoencoders. *npj Computational Materials*, 10(1): 139, 2024.
- Jin, W., Barzilay, R., and Jaakkola, T. Junction tree variational autoencoder for molecular graph generation. *35th International Conference on Machine Learning, ICML 2018*, 5:3632–3648, 2018.
- Klamt, A., Eckert, F., and Arlt, W. COSMO-RS: An Alternative to Simulation for Calculating Thermodynamic Properties of Liquid Mixtures. *Annual Review of Chemical and Biomolecular Engineering*, 1(1):101–122, jun 2010. ISSN 1947-5438. doi: 10.1146/annurev-chembioeng-073009-100903.
- König-Mattern, L., Medina, E. I. S., Komarova, A. O., Linke, S., Rihko-Struckmann, L., Luterbacher, J. S., and Sundmacher, K. Machine learning-supported solvent design for lignin-first biorefineries and lignin upgrading. *Chemical Engineering Journal*, 495:153524, 2024.
- Kool, W., Van Hoof, H., and Welling, M. Stochastic beams and where to find them: The gumbel-top-k trick for sampling sequences without replacement. In *International Conference on Machine Learning*, pp. 3499–3508. PMLR, 2019.
- Krenn, M., Häse, F., Nigam, A., Friederich, P., and Aspuru-Guzik, A. Self-referencing embedded strings (selfies): A 100% robust molecular string representation. *Machine Learning: Science and Technology*, 1(4):045024, 2020.
- Li, Y., Zhang, L., and Liu, Z. Multi-objective de novo drug design with conditional graph generative model. *Journal of cheminformatics*, 10:1–24, 2018.
- Mahmood, O., Mansimov, E., Bonneau, R., and Cho, K. Masked graph modeling for molecule generation. *Nature communications*, 12(1):3156, 2021.
- Maziarka, Ł., Danel, T., Mucha, S., Rataj, K., Tabor, J., and Jastrzebski, S. Molecule-augmented attention transformer. In *Workshop on Graph Representation Learning, Neural Information Processing Systems*, 2019.
- Mazuz, E., Shtar, G., Shapira, B., and Rokach, L. Molecule generation using transformers and policy gradient reinforcement learning. *Scientific Reports*, 13(1):8799, 2023.
- Medina, E. I. S., Linke, S., Stoll, M., and Sundmacher, K. Gibbs–helmholtz graph neural network: capturing the temperature dependency of activity coefficients at infinite dilution. *Digital Discovery*, 2(3):781–798, 2023. doi: 10.1039/d2dd00142j. URL <https://doi.org/10.1039/d2dd00142j>.
- Mnih, V. Playing atari with deep reinforcement learning. *arXiv preprint arXiv:1312.5602*, 2013.
- Nevolianis, T., Rittig, J. G., Mitsos, A., and Leonhard, K. Multi-fidelity graph neural networks for predicting toluene/water partition coefficients. *ChemRxiv preprint 10.26434/chemrxiv-2024-3t818*, 2024.
- Nigam, A., Pollice, R., Krenn, M., dos Passos Gomes, G., and Aspuru-Guzik, A. Beyond generative models: superfast traversal, optimization, novelty, exploration and discovery (stoned) algorithm for molecules using selfies. *Chemical science*, 12(20):7079–7090, 2021.
- Nigam, A., Pollice, R., Tom, G., Jorner, K., Willes, J., Thiede, L., Kundaje, A., and Aspuru-Guzik, A. Tartarus: A benchmarking platform for realistic and practical inverse molecular design. *Advances in Neural Information Processing Systems*, 36:3263–3306, 2023.
- Nnadili, M., Okafor, A. N., Olayiwola, T., Akinpelu, D., Kumar, R., and Romagnoli, J. A. Surfactant-specific ai-driven molecular design: Integrating generative models, predictive modeling, and reinforcement learning for tailored surfactant synthesis. *Industrial & Engineering Chemistry Research*, 63(14):6313–6324, 2024.
- O’Boyle, N. and Dalke, A. Deepsmiles: an adaptation of smiles for use in machine-learning of chemical structures. 2018.
- Olivecrona, M., Blaschke, T., Engkvist, O., and Chen, H. Molecular de-novo design through deep reinforcement learning. *Journal of cheminformatics*, 9:1–14, 2017.
- Peters, M., Zavrel, M., Kahlen, J., Schmidt, T., Ansorge-Schumacher, M., Leitner, W., Büchs, J., Greiner, L., and Spiess, A. C. Systematic approach to solvent selection for biphasic systems with a combination of cosmo–rs and a dynamic modeling tool. *Engineering in Life Sciences*, 8(5):546–552, 2008. ISSN 1618-0240. doi: 10.1002/elsc.200800037.
- Pirnay, J. and Grimm, D. G. Self-improvement for neural combinatorial optimization: Sample without replacement, but improvement. *Transactions on Machine Learning Research*, 2024a. ISSN 2835-8856. URL <https://openreview.net/forum?id=agT8ojoH0X>. Featured Certification.
- Pirnay, J. and Grimm, D. G. Take a step and reconsider: Sequence decoding for self-improved neural combinatorial optimization. *arXiv preprint arXiv:2407.17206*, 2024b.

- Reiser, P., Neubert, M., Eberhard, A., Torresi, L., Zhou, C., Shao, C., Metni, H., van Hoesel, C., Schopmans, H., Sommer, T., and Friederich, P. Graph neural networks for materials science and chemistry. *Communications Materials*, 3(1):93, 2022. doi: 10.1038/s43246-022-00315-6.
- Rittig, J. G. and Mitsos, A. Thermodynamics-consistent graph neural networks. *Chemical Science*, 2024. doi: 10.1039/d4sc04554h.
- Rittig, J. G., Ben Hicham, K., Schweidtmann, A. M., Dahmen, M., and Mitsos, A. Graph neural networks for temperature-dependent activity coefficient prediction of solutes in ionic liquids. *Computers and Chemical Engineering*, 171:108153, 2023a. ISSN 00981354. doi: 10.1016/j.compchemeng.2023.108153. URL <https://doi.org/10.1016/j.compchemeng.2023.108153>.
- Rittig, J. G., Felton, K. C., Lapkin, A. A., and Mitsos, A. Gibbs-Duhem-informed neural networks for binary activity coefficient prediction. *Digital Discovery*, 2:1752–1767, 2023b. doi: 10.1039/D3DD00103B. URL <https://doi.org/10.1039/D3DD00103B>.
- Rittig, J. G., Gao, Q., Dahmen, M., Mitsos, A., and Schweidtmann, A. M. Graph neural networks for the prediction of molecular structure–property relationships. In Zhang, D. and Del Río Chanona, E. A. (eds.), *Machine Learning and Hybrid Modelling for Reaction Engineering*, pp. 159–181. Royal Society of Chemistry, 2023c. ISBN 978-1-83916-563-4. doi: 10.1039/BK9781837670178-00159.
- Rittig, J. G., Ritzert, M., Schweidtmann, A. M., Winkler, S., Weber, J. M., Morsch, P., Heufer, K. A., Grohe, M., Mitsos, A., and Dahmen, M. Graph machine learning for design of high-octane fuels. *AIChE journal*, 69(4): e17971, 2023d.
- Sanchez-Lengeling, B. and Aspuru-Guzik, A. Inverse molecular design using machine learning: Generative models for matter engineering. *Science*, 361(6400):360–365, 2018.
- Sarathy, S. M. and Eraqi, B. A. Artificial intelligence for novel fuel design. *Proceedings of the Combustion Institute*, 40(1-4):105630, 2024.
- Schilter, O., Vaucher, A., Schwaller, P., and Laino, T. Designing catalysts with deep generative models and computational data. a case study for suzuki cross coupling reactions. *Digital discovery*, 2(3):728–735, 2023.
- Schneider, G. and Fechner, U. Computer-based de novo design of drug-like molecules. *Nature Reviews Drug Discovery*, 4(8):649–663, 2005.
- Schulman, J., Wolski, F., Dhariwal, P., Radford, A., and Klimov, O. Proximal policy optimization algorithms. *arXiv preprint arXiv:1707.06347*, 2017.
- Segler, M. H., Kogej, T., Tyrchan, C., and Waller, M. P. Generating focused molecule libraries for drug discovery with recurrent neural networks. *ACS central science*, 4(1):120–131, 2018.
- Shi, K., Bieber, D., and Sutton, C. Incremental sampling without replacement for sequence models. In *International Conference on Machine Learning*, pp. 8785–8795. PMLR, 2020.
- Skinnider, M. A. Invalid smiles are beneficial rather than detrimental to chemical language models. *Nature Machine Intelligence*, 6(4):437–448, 2024.
- Specht, T., Nagda, M., Fellenz, S., Mandt, S., Hasse, H., and Jirasek, F. Hanna: Hard-constraint neural network for consistent activity coefficient prediction. *arXiv preprint arXiv:2407.18011*, 2024.
- Steinborn, C., Huber, T., Lichtenegger, J., Plangger, I., Höfler, D., Schnell, S. D., Weisheit, L., Mayer, P., Wurst, K., and Magauer, T. Synthesis of waixenicin a: Exploring strategies for nine-membered ring formation. *Chemistry – A European Journal*, 30(7):e202303489, December 2023. ISSN 1521-3765. doi: 10.1002/chem.202303489. URL <http://dx.doi.org/10.1002/chem.202303489>.
- Vaswani, A. Attention is all you need. *Advances in Neural Information Processing Systems*, 2017.
- Wagner, A. Z. Constructions in combinatorics via neural networks. *arXiv preprint arXiv:2104.14516*, 2021.
- Wang, Y., Li, Z., and Barati Farimani, A. Graph neural networks for molecules. In *Machine Learning in Molecular Sciences*, pp. 21–66. Springer, 2023.
- Weininger, D. Smiles, a chemical language and information system. 1. introduction to methodology and encoding rules. *Journal of Chemical Information and Computer Sciences*, 28(1):31–36, 1988. doi: 10.1021/ci00057a005. URL <https://doi.org/10.1021/ci00057a005>.
- Williams, R. J. Simple statistical gradient-following algorithms for connectionist reinforcement learning. *Machine learning*, 8:229–256, 1992.
- Winter, B., Winter, C., Schilling, J., and Bardow, A. A smile is all you need: predicting limiting activity coefficients from SMILES with natural language processing. *Digital Discovery*, 1:859–869, 2022. doi: 10.1039/d2dd00058j.



- Winter, B., Winter, C., Esper, T., Schilling, J., and Bardow, A. Spt-nrtl: A physics-guided machine learning model to predict thermodynamically consistent activity coefficients. *Fluid Phase Equilibria*, 568:113731, 2023. ISSN 03783812. doi: 10.1016/j.fluid.2023.113731.
- Wisniak, J. Liquid—liquid phase splitting—i analytical models for critical mixing and azeotropy. *Chemical Engineering Science*, 38(6):969–978, 1983.
- Xu, P., Fu, T., Gao, W., and Sun, J. REINVENT-transformer: Molecular de novo design through transformer-based reinforcement learning. In *Artificial Intelligence and Data Science for Healthcare: Bridging Data-Centric AI and People-Centric Healthcare*, 2024. URL <https://openreview.net/forum?id=XykiSFid41>.
- Ying, C., Cai, T., Luo, S., Zheng, S., Ke, G., He, D., Shen, Y., and Liu, T.-Y. Do transformers really perform badly for graph representation? *Advances in neural information processing systems*, 34:28877–28888, 2021.
- Yue, T., Tao, L., Varshney, V., and Li, Y. Benchmarking study of deep generative models for inverse polymer design. *ChemRxiv*, 2024.
- Zamora, W. J., Viayna, A., Pinheiro, S., Curutchet, C., Bisbal, L., Ruiz, R., Ràfols, C., and Luque, F. J. Prediction of toluene/water partition coefficients in the sampl9 blind challenge: assessment of machine learning and iefpcm/mst continuum solvation models. *Physical Chemistry Chemical Physics*, pp. 10.1039/D3CP01428B, 2023. doi: 10.1039/D3CP01428B. URL <http://dx.doi.org/10.1039/D3CP01428B>.
- Zang, C. and Wang, F. Moflow: an invertible flow model for generating molecular graphs. In *Proceedings of the 26th ACM SIGKDD international conference on knowledge discovery & data mining*, pp. 617–626, 2020.
- Zhang, X., Wang, L., Helwig, J., Luo, Y., Fu, C., Xie, Y., Liu, M., Lin, Y., Xu, Z., Yan, K., et al. Artificial intelligence for science in quantum, atomistic, and continuum systems. *arXiv preprint arXiv:2307.08423*, 2023a.
- Zhang, Z., Liu, Q., Lee, C.-K., Hsieh, C.-Y., and Chen, E. An equivariant generative framework for molecular graph-structure co-design. *Chemical Science*, 14(31): 8380–8392, 2023b.
- Zhou, Z., Kearnes, S., Li, L., Zare, R. N., and Riley, P. Optimization of molecules via deep reinforcement learning. *Scientific reports*, 9(1):10752, 2019.